

# Redetermination of the crystal structure of $\text{RhPb}_2$ from single-crystal X-ray diffraction data, revealing a rhodium deficiency

Takashi Mochiku,<sup>a\*</sup> Yoshitaka Matsushita,<sup>a</sup> Nikola Subotić,<sup>b</sup> Takanari Kashiwagi<sup>b</sup> and Kazuo Kadowaki<sup>b</sup>

Received 18 October 2021

Accepted 19 November 2021

Edited by M. Weil, Vienna University of Technology, Austria

**Keywords:** crystal structure; rhodium; lead; intermetallic compound; deficiency; superconductivity.

**CCDC reference:** 2123239

**Supporting information:** this article has supporting information at journals.iucr.org/e

<sup>a</sup>National Institute for Materials Science, 1-2-1 Sengen, Tsukuba, Ibaraki 305-0047, Japan, and <sup>b</sup>University of Tsukuba, 1-1 Tennouda, Tsukuba, Ibaraki 305-8573, Japan. \*Correspondence e-mail: mochiku.takashi@nims.go.jp

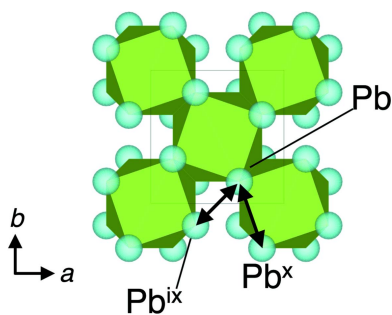
$\text{RhPb}_2$  (rhodium dilead) is a superconductor crystallizing in the  $\text{CuAl}_2$  structure type (space group  $I4/mcm$ ). The Rh and Pb atoms are located at the  $4a$  (site symmetry  $422$ ) and  $8h$  ( $m.2m$ ) sites, respectively. The crystal structure is composed of  $[\text{RhPb}_8]$  antiprisms, which share their square faces along the  $c$  axis and the edges in the direction perpendicular to the  $c$  axis. We have succeeded in growing single crystals of  $\text{RhPb}_2$  and have re-determined the crystal structure on basis of single-crystal X-ray diffraction data. In comparison with the previous structure studies using powder X-ray diffraction data [Wallbaum (1943). *Z. Metallkd.* **35**, 218–221; Havinga *et al.* (1972). *J. Less-Common Met.* **27**, 169–186], the current structure analysis of  $\text{RhPb}_2$  leads to more precise unit-cell parameters and fractional coordinates, together with anisotropic displacement parameters for the two atoms. In addition and likewise different from the previous studies, we have found a slight deficiency of Rh in  $\text{RhPb}_2$ , leading to a refined formula of  $\text{Rh}_{0.950(9)}\text{Pb}_2$ .

## 1. Chemical context

A large number of binary intermetallic compounds with the  $\text{CuAl}_2$  structure type have been reported (Wallbaum, 1943; Havinga *et al.*, 1972; Havinga, 1972), and several of them exhibit superconductivity (Gendron & Jones, 1962).  $\text{RhPb}_2$  is one of them, with a superconducting transition temperature ( $T_c$ ) of 2.66 K (Gendron & Jones, 1962).  $\beta$ - $\text{RhPb}_2$  adopting the  $\beta$ - $\text{PdBi}_2$  structure type (space group  $I4/mmm$ ) has been reported as a candidate material for topological superconductors (Zhang *et al.*, 2019), and  $\text{RhPb}_2$  crystallizing in the  $\text{CuAl}_2$  structure type has also attracted much attention. While the previous powder X-ray studies of  $\text{RhPb}_2$  (Wallbaum, 1943; Havinga *et al.*, 1972) used polycrystalline material prepared by a melting method, we have grown  $\text{RhPb}_2$  single crystals by application of a vertical pulling mechanism using an infrared mirror furnace. Here we report on the redetermined crystal structure of  $\text{RhPb}_2$  based on single-crystal X-ray data.

## 2. Structural commentary

The crystal structure of  $\text{RhPb}_2$  refined from single-crystal data is essentially the same as determined previously (Wallbaum, 1943; Havinga *et al.*, 1972).  $\text{RhPb}_2$  is composed of  $[\text{RhPb}_8]$  antiprisms, which share the square faces along the  $c$  axis and the edges in the direction perpendicular to the  $c$  axis (Fig. 1).



OPEN ACCESS

The Rh atom (site symmetry 422) is surrounded by eight Pb atoms occupying the edges of the  $[\text{RhPb}_8]$  antiprism, and two Rh atoms are spaced along the  $c$  axis at a distance of half of the unit-cell parameter  $c$ . The Pb–Pb distance in the adjacent  $[\text{RhPb}_8]$  antiprism is the shortest among the Pb–Pb distances

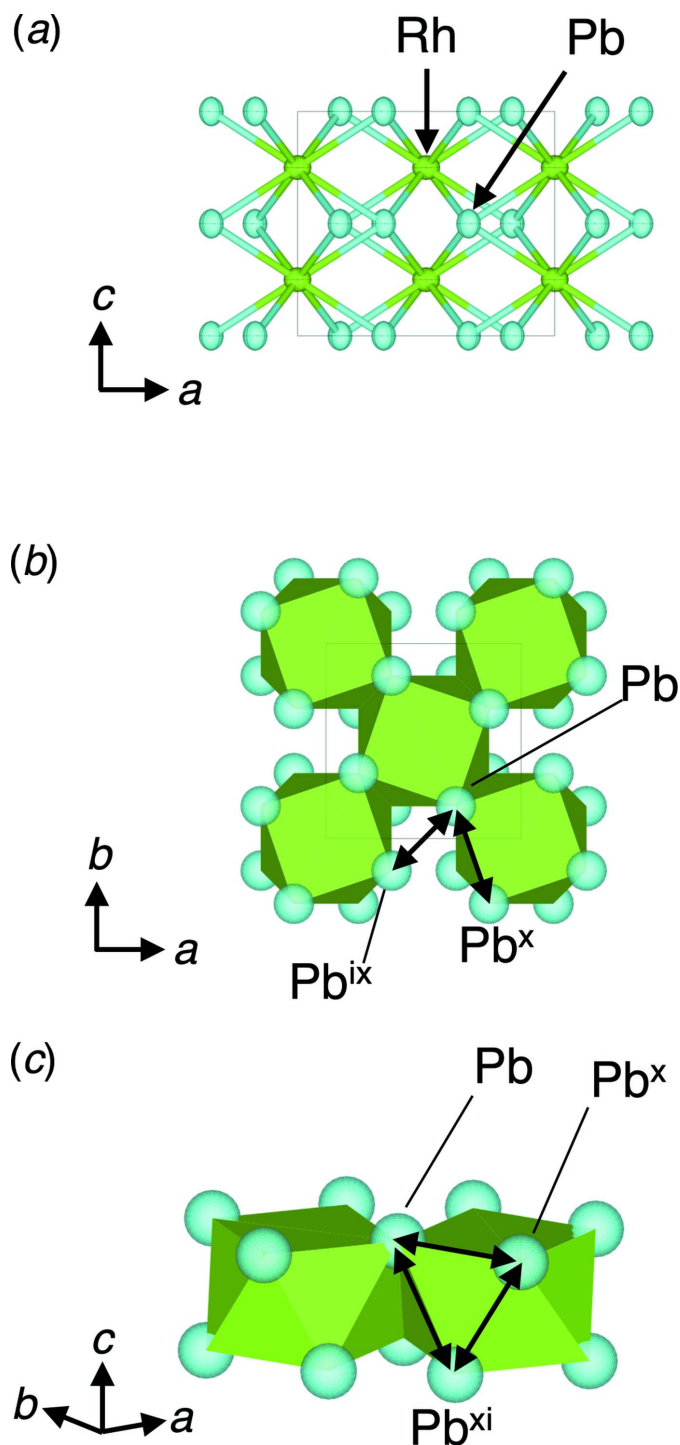


**Figure 1**  
 (a) The crystal structure of  $\text{RhPb}_2$  in a view along the  $b$  axis showing the atoms in the asymmetric unit with displacement ellipsoids at the 99.9%; (b) the crystal structure of  $\text{RhPb}_2$  in polyhedral representation in a view along the  $c$  axis; (c) details of the linkage of the  $[\text{RhPb}_8]$  antiprisms in the crystal structure of  $\text{RhPb}_2$ .

**Table 1**

Comparison of unit-cell parameters and interatomic distances ( $\text{\AA}$ ) at room temperature in  $\text{RhPb}_2$  determined in previous and the present studies.

	Wallbaum (1943)	Havinga <i>et al.</i> (1972)	This work
$a$	6.651 (3)	6.674 (3)	6.7068 (4)
$c$	5.853 (3)	5.831 (3)	5.8623 (6)
Rh–Pb	2.902	2.885 (6)	2.9016 (2)
Pb–Pb <sup>ix</sup>	2.972	3.134 (14)	3.1313 (13)
Pb–Pb <sup>x</sup>	3.544	3.520 (10)	3.5416 (4)
Pb–Pb <sup>xi</sup>	3.603	3.662 (9)	3.6734 (6)
Pb <sup>x</sup> –Pb <sup>xi</sup>	3.400	3.319 (7)	3.3448 (7)

Symmetry codes: (ix)  $-x + 1, -y, -z + 1$ ; (x)  $-y + 1, x - 1, z$ ; (xi)  $y + \frac{1}{2}, -x + \frac{1}{2}, -z + \frac{1}{2}$ .

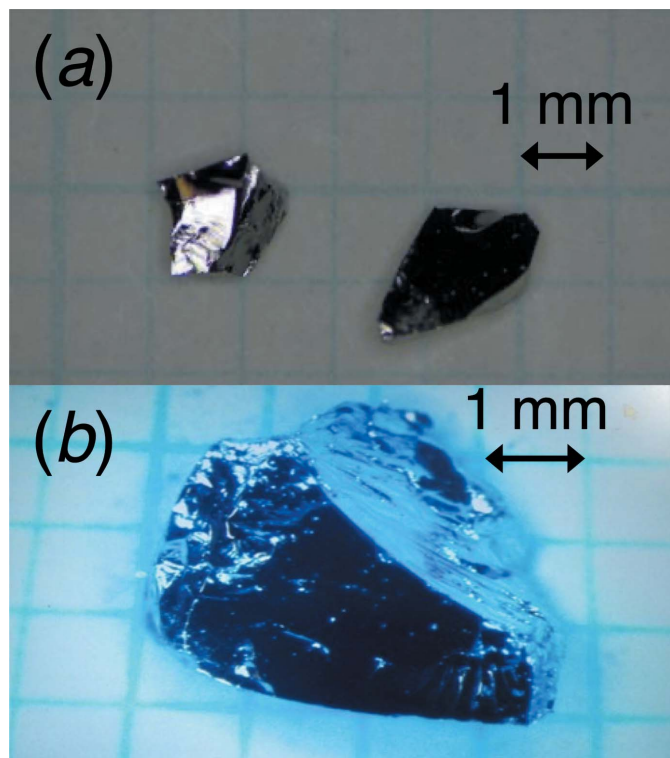
(Table 1; Fig. 1b, Pb–Pb<sup>ix</sup>); all Pb–Pb distances belonging to the shared square faces of the  $[\text{RhPb}_8]$  antiprism are equal (Fig. 1b, Pb–Pb<sup>x</sup>), while the Pb–Pb distances belonging to the sides of the triangle of the  $[\text{RhPb}_8]$  antiprism are all different (Fig. 1c, Pb–Pb<sup>x</sup>, Pb–Pb<sup>xi</sup> and Pb<sup>x</sup>–Pb<sup>xi</sup>).

While  $\text{RhPb}_2$  has been reported to be single phase only in a Pb-deficient sample (Havinga *et al.*, 1972), we have found a deficiency of Rh rather than a deficiency of Pb in the grown single crystals. The chemical composition obtained from the analysis of the occupancy of Rh is  $\text{Rh}_{0.950(9)}\text{Pb}_2$ . Hamilton's  $R$ -factor ratio test (Hamilton, 1965) was used to compare the  $R$  factors for the models with and without a deficiency of Rh. The result rejected the model without deficiency of Rh at a significance level of less than 0.005.

Table 1 shows the unit-cell parameters and interatomic distances obtained from the current and the previous studies (Wallbaum, 1943; Havinga *et al.*, 1972). The unit-cell parameters are more precise and larger than those of the previous studies, and the free fractional coordinate of Rh was also obtained with higher precision. The resulting interatomic distances are slightly different from those in the previous studies. Anisotropic displacement parameters, which were not reported previously, were also obtained from the current redetermination.

### 3. Synthesis and crystallization

Single crystals of  $\text{RhPb}_2$  were grown from the Pb-rich melt (molar ratio Rh:Pb = 1:8) by a slow cooling process in a steep temperature gradient infrared furnace according to the Pb–Rh binary phase diagram (El-Boragy *et al.*, 1992), where  $\text{RhPb}_2$  is shown to grow through the peritectic reaction incongruently melting between 593 and 913 K. The raw materials of Rh and Pb were of 99.9% purity in powder form (300 mesh) and 99.99% in shots, respectively, purchased from Furuuchi Chemical Co. Prior to crystal growth, Rh and Pb were melted together in an evacuated silica tube by heating with a flame torch. The obtained ingot was then put into a new silica tube and was vacuum sealed. The silica tube was hung in an infrared mirror furnace, which generally has a strong temperature gradient around the focal point. The sample silica tube was heated above 913 K, where the sample became completely liquid. Then, the silica tube was placed at the


**Figure 2**

(a) A photograph of two pieces of single crystals of  $\text{RhPb}_2$  taken under an optical microscope; (b) an enlarged optical photograph of one of the single-crystals of  $\text{RhPb}_2$ .

position where the temperature gradient is the highest. The silica tube was rotated slowly ( $\sim 10$  r.p.m.) to promote single crystals to grow in a uniform temperature horizontally with a steep temperature gradient vertically. A silica tube with a cone-shaped bottom was used. The furnace temperature was slowly decreased with a constant rate of  $0.5 \text{ K h}^{-1}$  until it reached the temperature well below  $593 \text{ K}$ , then it was lowered to room temperature.

After removing the silica tube carefully, the grown boule showed clearly the liquid–solid phase boundary as a horizontal line in the upper part of the boule, indicating that the single-crystal growth had progressed as planned according to the phase diagram (El-Boragy *et al.*, 1992). More than half of the grown boule from the bottom appeared to have turned into a single crystal of  $\text{RhPb}_2$ . The latter cleaves easily, showing shiny reflection with a silvery luster from the cleaved surface. The single crystal was rather soft and could easily be scratched by tweezers. The product seems to be stable in air because the color of the cleaved surface did not change over time. In Fig. 2 photographs of the grown single crystals of  $\text{RhPb}_2$  are shown.

#### 4. Refinement

Crystal data, data collection and structure refinement details are summarized in Table 2. The equivalent isotropic atomic displacement parameter ( $U_{\text{eq}}$ ) of the Rh sites for the model without deficiency of Rh was  $0.0131 (5) \text{ \AA}^2$ , which was larger than that of Pb ( $0.0107 (3) \text{ \AA}^2$ ). We refined the occupancies of

**Table 2**

Experimental details.

Crystal data	
Chemical formula	$\text{Rh}_{0.95}\text{Pb}_2$
$M_r$	512.14
Crystal system, space group	Tetragonal, $I4/mcm$
Temperature (K)	295
$a, c$ ( $\text{\AA}$ )	6.7068 (4), 5.8623 (6)
$V$ ( $\text{\AA}^3$ )	263.69 (4)
$Z$	4
Radiation type	Mo $K\alpha$
$\mu$ ( $\text{mm}^{-1}$ )	132.87
Crystal size (mm)	$0.11 \times 0.05 \times 0.03$
Data collection	
Diffractometer	XtaLAB Mini II
Absorption correction	Multi-scan ( <i>CrysAlis PRO</i> ; Rigaku OD, 2019)
$T_{\text{min}}, T_{\text{max}}$	0.123, 1.000
No. of measured, independent and observed [ $I > 2\sigma(I)$ ] reflections	461, 117, 88
$R_{\text{int}}$	0.033
$(\sin \theta/\lambda)_{\text{max}}$ ( $\text{\AA}^{-1}$ )	0.708
Refinement	
$R[F^2 > 2\sigma(F^2)], wR(F^2), S$	0.021, 0.042, 1.01
No. of reflections	117
No. of parameters	9
$\Delta\rho_{\text{max}}, \Delta\rho_{\text{min}}$ ( $\text{e \AA}^{-3}$ )	1.96, $-1.56$

Computer programs: *CrysAlis PRO* (Rigaku OD, 2019), *SHELXT* (Sheldrick, 2015a), *SHELXL* (Sheldrick, 2015b) and *OLEX2* (Dolomanov *et al.*, 2009).

Rh and Pb. While the refined occupancy of Pb was very close to full occupation, the refined occupancy of Rh indicated a significant deficiency of this site. The final  $wR(F^2)$  value for the model without deficiency of Rh was 0.047, and that for the model with deficiency of Rh was 0.042. In the final model [occupancy of Rh = 0.950 (9); full occupancy of Pb] the atomic displacement parameter ( $U_{\text{eq}}$ ) of the Rh site is the same as that of the Pb site.

#### Funding information

Funding for this research was provided by: Japan Society for the Promotion of Science (grant No. JP19H05819).

#### References

- Dolomanov, O. V., Bourhis, L. J., Gildea, R. J., Howard, J. A. K. & Puschmann, H. (2009). *J. Appl. Cryst.* **42**, 339–341.
- El-Boragy, M., Jain, K. C., Mayer, H. W. & Schubert, K. (1992). *Z. Metallkd.* **63**, 751.
- Gendron, M. F. & Jones, R. E. (1962). *J. Phys. Chem. Solids*, **23**, 405–406.
- Hamilton, W. C. (1965). *Acta Cryst.* **18**, 502–510.
- Havinga, E. E. (1972). *J. Less-Common Met.* **27**, 187–193.
- Havinga, E. E., Damsma, H. & Hokkeling, P. (1972). *J. Less-Common Met.* **27**, 169–186.
- Rigaku OD (2019). *CrysAlis PRO*. Rigaku Oxford Diffraction, Yarnton, England.
- Sheldrick, G. M. (2015a). *Acta Cryst.* **A71**, 3–8.
- Sheldrick, G. M. (2015b). *Acta Cryst.* **C71**, 3–8.
- Wallbaum, H. J. (1943). *Z. Metallkd.* **35**, 218–221.
- Zhang, J., Guo, P., Gao, M., Liu, K. & Lu, Z. (2019). *Phys. Rev. B*, **99**, 045110.

## supporting information

*Acta Cryst.* (2021). E77, 1327-1329 [https://doi.org/10.1107/S2056989021012275]

## Redetermination of the crystal structure of $\text{RhPb}_2$ from single-crystal X-ray diffraction data, revealing a rhodium deficiency

Takashi Mochiku, Yoshitaka Matsushita, Nikola Subotić, Takanari Kashiwagi and Kazuo Kadowaki

### Computing details

Data collection: *CrysAlis PRO* (Rigaku OD, 2019); cell refinement: *CrysAlis PRO* (Rigaku OD, 2019); data reduction: *CrysAlis PRO* (Rigaku OD, 2019); program(s) used to solve structure: ShelXT (Sheldrick, 2015a); program(s) used to refine structure: *SHELXL* (Sheldrick, 2015b); molecular graphics: *OLEX2* (Dolomanov *et al.*, 2009); software used to prepare material for publication: *OLEX2* (Dolomanov *et al.*, 2009).

### Rhodium dilead

#### Crystal data

$\text{Rh}_{0.95}\text{Pb}_2$

$M_r = 512.14$

Tetragonal, *I4/mcm*

$a = 6.7068$  (4) Å

$c = 5.8623$  (6) Å

$V = 263.69$  (4) Å<sup>3</sup>

$Z = 4$

$F(000) = 827$

$D_x = 12.900$  Mg m<sup>-3</sup>

Mo  $K\alpha$  radiation,  $\lambda = 0.71073$  Å

Cell parameters from 295 reflections

$\theta = 6.1\text{--}30.2^\circ$

$\mu = 132.87$  mm<sup>-1</sup>

$T = 295$  K

Irregular, metallic dark grey

$0.11 \times 0.05 \times 0.03$  mm

#### Data collection

XtaLAB Mini II

diffractometer

Detector resolution: 10.0000 pixels mm<sup>-1</sup>

$\omega$  scans

Absorption correction: multi-scan

(*CrysAlisPro*; Rigaku OD, 2019)

$T_{\min} = 0.123$ ,  $T_{\max} = 1.000$

461 measured reflections

117 independent reflections

88 reflections with  $I > 2\sigma(I)$

$R_{\text{int}} = 0.033$

$\theta_{\max} = 30.2^\circ$ ,  $\theta_{\min} = 4.3^\circ$

$h = -9 \rightarrow 8$

$k = -7 \rightarrow 9$

$l = -8 \rightarrow 7$

#### Refinement

Refinement on  $F^2$

Least-squares matrix: full

$R[F^2 > 2\sigma(F^2)] = 0.021$

$wR(F^2) = 0.042$

$S = 1.01$

117 reflections

9 parameters

0 restraints

Primary atom site location: iterative

$w = 1/[\sigma^2(F_o^2) + (0.013P)^2]$

where  $P = (F_o^2 + 2F_c^2)/3$

$(\Delta/\sigma)_{\max} < 0.001$

$\Delta\rho_{\max} = 1.96$  e Å<sup>-3</sup>

$\Delta\rho_{\min} = -1.56$  e Å<sup>-3</sup>

Extinction correction: SHELXL2018/3

(Sheldrick 2015b),

$F_c^* = kF_c[1 + 0.001 \times F_c^2 \lambda^3 / \sin(2\theta)]^{-1/4}$

Extinction coefficient: 0.0030 (3)

*Special details*

**Geometry.** All esds (except the esd in the dihedral angle between two l.s. planes) are estimated using the full covariance matrix. The cell esds are taken into account individually in the estimation of esds in distances, angles and torsion angles; correlations between esds in cell parameters are only used when they are defined by crystal symmetry. An approximate (isotropic) treatment of cell esds is used for estimating esds involving l.s. planes.

*Fractional atomic coordinates and isotropic or equivalent isotropic displacement parameters ( $\text{\AA}^2$ )*

	<i>x</i>	<i>y</i>	<i>z</i>	$U_{\text{iso}}^*/U_{\text{eq}}$	Occ. (<1)
Rh	0.500000	0.500000	0.750000	0.0103 (7)	0.950 (9)
Pb	0.66507 (7)	0.16507 (7)	0.500000	0.0103 (3)	

*Atomic displacement parameters ( $\text{\AA}^2$ )*

	$U^{11}$	$U^{22}$	$U^{33}$	$U^{12}$	$U^{13}$	$U^{23}$
Rh	0.0111 (8)	0.0111 (8)	0.0088 (11)	0.000	0.000	0.000
Pb	0.0091 (3)	0.0091 (3)	0.0128 (4)	0.0013 (3)	0.000	0.000

*Geometric parameters ( $\text{\AA}$ ,  $^\circ$ )*

Rh—Rh <sup>i</sup>	2.9312 (3)	Rh—Pb <sup>viii</sup>	2.9016 (2)
Rh—Rh <sup>ii</sup>	2.9312 (3)	Pb—Pb <sup>ix</sup>	3.1313 (13)
Rh—Pb <sup>iii</sup>	2.9016 (2)	Pb—Pb <sup>x</sup>	3.5416 (4)
Rh—Pb <sup>iv</sup>	2.9016 (2)	Pb—Pb <sup>xi</sup>	3.6734 (6)
Rh—Pb <sup>ii</sup>	2.9016 (2)	Pb—Pb <sup>xii</sup>	3.5416 (4)
Rh—Pb	2.9016 (2)	Pb—Pb <sup>iv</sup>	3.5416 (4)
Rh—Pb <sup>v</sup>	2.9016 (2)	Pb—Pb <sup>vii</sup>	3.5416 (4)
Rh—Pb <sup>vi</sup>	2.9016 (2)	Pb—Pb <sup>xiii</sup>	3.3448 (7)
Rh—Pb <sup>vii</sup>	2.9016 (2)	Pb—Pb <sup>v</sup>	3.3448 (7)
Rh <sup>ii</sup> —Rh—Rh <sup>i</sup>	180.0	Rh <sup>v</sup> —Pb—Pb <sup>xi</sup>	99.966 (13)
Pb <sup>ii</sup> —Rh—Rh <sup>i</sup>	59.663 (4)	Rh <sup>xiv</sup> —Pb—Pb <sup>x</sup>	52.390 (2)
Pb—Rh—Rh <sup>i</sup>	120.337 (4)	Rh <sup>ii</sup> —Pb—Pb <sup>xii</sup>	96.44 (2)
Pb <sup>iii</sup> —Rh—Rh <sup>i</sup>	59.663 (4)	Rh <sup>xiv</sup> —Pb—Pb <sup>iv</sup>	148.841 (9)
Pb <sup>iv</sup> —Rh—Rh <sup>i</sup>	120.337 (4)	Rh <sup>v</sup> —Pb—Pb <sup>xii</sup>	52.390 (2)
Pb <sup>vi</sup> —Rh—Rh <sup>i</sup>	59.663 (4)	Rh <sup>xiv</sup> —Pb—Pb <sup>xi</sup>	50.729 (10)
Pb <sup>viii</sup> —Rh—Rh <sup>i</sup>	59.663 (4)	Rh <sup>v</sup> —Pb—Pb <sup>vii</sup>	96.44 (2)
Pb <sup>vii</sup> —Rh—Rh <sup>ii</sup>	59.663 (4)	Rh—Pb—Pb <sup>xii</sup>	96.44 (2)
Pb <sup>vi</sup> —Rh—Rh <sup>ii</sup>	120.337 (4)	Rh—Pb—Pb <sup>x</sup>	148.842 (9)
Pb <sup>iii</sup> —Rh—Rh <sup>ii</sup>	120.337 (4)	Rh <sup>v</sup> —Pb—Pb <sup>xiii</sup>	107.993 (18)
Pb—Rh—Rh <sup>ii</sup>	59.663 (4)	Rh <sup>ii</sup> —Pb—Pb <sup>ix</sup>	106.118 (12)
Pb <sup>vii</sup> —Rh—Rh <sup>i</sup>	120.337 (4)	Rh—Pb—Pb <sup>ix</sup>	106.118 (12)
Pb <sup>v</sup> —Rh—Rh <sup>ii</sup>	120.337 (4)	Rh <sup>xiv</sup> —Pb—Pb <sup>vii</sup>	96.44 (2)
Pb <sup>v</sup> —Rh—Rh <sup>i</sup>	59.663 (4)	Rh <sup>v</sup> —Pb—Pb <sup>ix</sup>	106.118 (12)
Pb <sup>viii</sup> —Rh—Rh <sup>ii</sup>	120.337 (4)	Rh <sup>ii</sup> —Pb—Pb <sup>x</sup>	148.841 (9)
Pb <sup>iv</sup> —Rh—Rh <sup>ii</sup>	59.663 (4)	Rh <sup>xiv</sup> —Pb—Pb <sup>ix</sup>	106.118 (12)
Pb <sup>ii</sup> —Rh—Rh <sup>i</sup>	120.337 (4)	Rh <sup>ii</sup> —Pb—Pb <sup>xi</sup>	93.646 (8)
Pb <sup>vii</sup> —Rh—Pb <sup>iii</sup>	135.14 (2)	Rh <sup>v</sup> —Pb—Pb <sup>v</sup>	54.805 (6)

Pb <sup>iv</sup> —Rh—Pb <sup>vii</sup>	119.326 (8)	Rh—Pb—Pb <sup>iv</sup>	52.390 (2)
Pb <sup>iv</sup> —Rh—Pb <sup>viii</sup>	70.390 (11)	Rh <sup>xiv</sup> —Pb—Pb <sup>v</sup>	107.993 (18)
Pb <sup>ii</sup> —Rh—Pb <sup>iii</sup>	70.390 (11)	Rh—Pb—Pb <sup>vii</sup>	52.390 (2)
Pb <sup>iv</sup> —Rh—Pb <sup>ii</sup>	75.220 (4)	Rh—Pb—Pb <sup>xiii</sup>	107.993 (18)
Pb <sup>iv</sup> —Rh—Pb <sup>v</sup>	135.14 (2)	Rh <sup>ii</sup> —Pb—Pb <sup>v</sup>	107.993 (18)
Pb—Rh—Pb <sup>viii</sup>	78.54 (2)	Rh <sup>ii</sup> —Pb—Pb <sup>xiii</sup>	54.805 (6)
Pb <sup>vii</sup> —Rh—Pb <sup>ii</sup>	75.220 (4)	Rh <sup>ii</sup> —Pb—Pb <sup>vii</sup>	52.390 (2)
Pb <sup>vi</sup> —Rh—Pb	135.14 (2)	Rh <sup>ii</sup> —Pb—Pb <sup>iv</sup>	52.390 (2)
Pb <sup>iv</sup> —Rh—Pb <sup>iii</sup>	78.54 (2)	Rh <sup>xiv</sup> —Pb—Pb <sup>xiii</sup>	54.805 (6)
Pb <sup>vi</sup> —Rh—Pb <sup>iii</sup>	75.220 (4)	Pb <sup>xiii</sup> —Pb—Pb <sup>vii</sup>	64.40 (2)
Pb <sup>viii</sup> —Rh—Pb <sup>ii</sup>	135.14 (2)	Pb <sup>v</sup> —Pb—Pb <sup>xii</sup>	64.40 (2)
Pb—Rh—Pb <sup>iii</sup>	147.76 (2)	Pb <sup>xii</sup> —Pb—Pb <sup>xi</sup>	101.180 (5)
Pb <sup>vi</sup> —Rh—Pb <sup>viii</sup>	119.326 (8)	Pb <sup>x</sup> —Pb—Pb <sup>iv</sup>	127.53 (3)
Pb <sup>viii</sup> —Rh—Pb <sup>iii</sup>	75.220 (3)	Pb <sup>ix</sup> —Pb—Pb <sup>xi</sup>	64.773 (7)
Pb <sup>iv</sup> —Rh—Pb	75.220 (3)	Pb <sup>vii</sup> —Pb—Pb <sup>xi</sup>	124.800 (14)
Pb <sup>iv</sup> —Rh—Pb <sup>vi</sup>	147.76 (2)	Pb <sup>xii</sup> —Pb—Pb <sup>iv</sup>	142.47 (3)
Pb—Rh—Pb <sup>vii</sup>	75.220 (3)	Pb <sup>iv</sup> —Pb—Pb <sup>xi</sup>	101.180 (5)
Pb—Rh—Pb <sup>ii</sup>	119.326 (8)	Pb <sup>vii</sup> —Pb—Pb <sup>xii</sup>	52.47 (3)
Pb <sup>viii</sup> —Rh—Pb <sup>vii</sup>	147.76 (2)	Pb <sup>ix</sup> —Pb—Pb <sup>vii</sup>	153.764 (14)
Pb <sup>v</sup> —Rh—Pb <sup>viii</sup>	75.220 (4)	Pb <sup>xiii</sup> —Pb—Pb <sup>xi</sup>	60.398 (9)
Pb <sup>vi</sup> —Rh—Pb <sup>ii</sup>	78.54 (2)	Pb <sup>ix</sup> —Pb—Pb <sup>x</sup>	63.764 (14)
Pb—Rh—Pb <sup>v</sup>	70.390 (12)	Pb <sup>v</sup> —Pb—Pb <sup>vii</sup>	64.40 (2)
Pb <sup>vi</sup> —Rh—Pb <sup>vii</sup>	70.390 (11)	Pb <sup>vii</sup> —Pb—Pb <sup>iv</sup>	90.0
Pb <sup>v</sup> —Rh—Pb <sup>ii</sup>	147.76 (2)	Pb <sup>ix</sup> —Pb—Pb <sup>v</sup>	118.80 (2)
Pb <sup>v</sup> —Rh—Pb <sup>iii</sup>	119.326 (8)	Pb <sup>v</sup> —Pb—Pb <sup>x</sup>	102.295 (2)
Pb <sup>v</sup> —Rh—Pb <sup>vii</sup>	78.54 (2)	Pb <sup>ix</sup> —Pb—Pb <sup>xiii</sup>	118.80 (2)
Pb <sup>vi</sup> —Rh—Pb <sup>v</sup>	75.220 (3)	Pb <sup>xiii</sup> —Pb—Pb <sup>xii</sup>	64.40 (2)
Rh—Pb—Rh <sup>v</sup>	109.610 (11)	Pb <sup>v</sup> —Pb—Pb <sup>xiii</sup>	122.41 (4)
Rh <sup>v</sup> —Pb—Rh <sup>ii</sup>	147.76 (2)	Pb <sup>xiii</sup> —Pb—Pb <sup>x</sup>	102.295 (2)
Rh—Pb—Rh <sup>ii</sup>	60.674 (7)	Pb <sup>ix</sup> —Pb—Pb <sup>xii</sup>	153.764 (14)
Rh <sup>ii</sup> —Pb—Rh <sup>xiv</sup>	109.610 (12)	Pb <sup>v</sup> —Pb—Pb <sup>xi</sup>	154.764 (7)
Rh—Pb—Rh <sup>xiv</sup>	147.76 (2)	Pb <sup>ix</sup> —Pb—Pb <sup>iv</sup>	63.764 (14)
Rh <sup>v</sup> —Pb—Rh <sup>xiv</sup>	60.674 (8)	Pb <sup>vii</sup> —Pb—Pb <sup>x</sup>	142.47 (3)
Rh <sup>v</sup> —Pb—Pb <sup>x</sup>	52.390 (2)	Pb <sup>v</sup> —Pb—Pb <sup>iv</sup>	102.295 (2)
Rh—Pb—Pb <sup>xi</sup>	150.417 (3)	Pb <sup>x</sup> —Pb—Pb <sup>xi</sup>	55.200 (14)
Rh—Pb—Pb <sup>v</sup>	54.805 (6)	Pb <sup>xiii</sup> —Pb—Pb <sup>iv</sup>	102.295 (2)
Rh <sup>v</sup> —Pb—Pb <sup>iv</sup>	148.841 (9)	Pb <sup>xii</sup> —Pb—Pb <sup>x</sup>	90.0
Rh <sup>xiv</sup> —Pb—Pb <sup>xii</sup>	52.390 (2)		

Symmetry codes: (i)  $-x+1, -y+1, -z+2$ ; (ii)  $-x+1, -y+1, -z+1$ ; (iii)  $x-1/2, y+1/2, z+1/2$ ; (iv)  $y, -x+1, -z+1$ ; (v)  $-x+3/2, -y+1/2, -z+3/2$ ; (vi)  $y+1/2, -x+3/2, -z+3/2$ ; (vii)  $-y+1, x, z$ ; (viii)  $-y+1/2, x-1/2, z+1/2$ ; (ix)  $-x+1, -y, -z+1$ ; (x)  $-y+1, x-1, z$ ; (xi)  $y+1/2, -x+1/2, -z+1/2$ ; (xii)  $y+1, -x+1, -z+1$ ; (xiii)  $-x+3/2, -y+1/2, -z+1/2$ ; (xiv)  $x+1/2, y-1/2, z-1/2$ .